Can. J. Remote Sensing, Vol. 30, No. 5, pp. 717–730, 2004

Soil water forecasting in the continental United States: relative forcing by meteorology versus leaf area index and the effects of meteorological forecast errors

Michael A. White and Ramakrishna R. Nemani

Abstract. Forecasts of the states and fluxes of terrestrial ecosystems are an increasingly important tool for a large fire, famine, irrigation, energy, recreation, and agriculture community. A detailed understanding of the relative importance of vegetation phenology and meteorology, two of the main forcings of ecosystem forecasts, and the likely impact of errors in phenological and (or) meteorological forecasts are required prior to management implementation. Using the terrestrial observation and prediction system (TOPS) and 1982–1997 leaf area index (LAI) and meteorology for the conterminous United States, we tested the relative importance of interannual variability in meteorology and LAI for soil water simulations. In nearly all cases, meteorological variability influenced simulations far more than did LAI; the effects of ignoring realistic variability in either variable were most pronounced in arid, low-LAI regions. We then identified the critical meteorological forecast errors in temperature and precipitation that were required to generate statistically significant differences in 1-week soil water forecasts. Temperature critical errors approached 10 °C in winter but were only about 2–3 °C in summer. Precipitation critical errors were much more constant throughout the year and were usually less than 1 cm (error in weekly total precipitation).

Résumé. Les estimations des états et des flux des écosystèmes terrestres constituent de plus en plus des outils importants pour l'importante communauté des spécialistes du feu, de la famine, de l'irrigation, de l'énergie, de la récréation et de l'agriculture. Il est essentiel d'avoir une connaissance détaillée de l'importance relative de la phénologie de la végétation et de la climatologie, deux des principaux éléments de forçage dans les estimations d'écosystèmes, et de l'impact probable des erreurs dans les estimations phénologiques et (ou) climatologiques avant de pouvoir mettre en place des politiques de gestion. À l'aide du système TOPS (« terrestrial observation and prediction system ») et des données LAI de 1982–1997 et des données climatiques des États-Unis continentaux, on a testé l'importance relative de la variabilité interannuelle de la climatologie et de LAI dans les simulations d'eau dans le sol. Dans presque tous les cas, la variabilité climatique avait une influence beaucoup plus grande sur les simulations que le LAI; le fait d'ignorer une variabilité réaliste dans l'une ou l'autre de ces variables avait une plus grande influence dans les régions arides présentant un indice LAI faible. Nous avons alors identifié les erreurs critiques dans les estimations climatiques au niveau de la température et des précipitations, nécessaires pour générer des différences statistiquement significatives dans les estimations d'eau dans le sol à l'échelle hebdomadaire. Les erreurs critiques au niveau de la température s'approchaient de 10 °C en hiver mais n'atteignaient qu'environ 2–3 °C en été. Les erreurs critiques dans le cas des précipitations étaient beaucoup plus constantes à travers l'année et étaient généralement de moins de 1 cm (erreur dans la précipitation hebdomadaire totale).
[Traduit par la Rédaction]

Introduction

Ecosystem fluxes of water and carbon are crucial determinants of the current and future state of the earth system. Weather, climate, stream flow, plant canopy water status, soil water resources, and carbon storage are all affected by short- to long-term variation in ecosystem fluxes. In addition to influences from human land cover modification (DeFries et al., 2002), edaphic conditions (Imhoff et al., 1997), and disturbance history (Thornton et al., 2002), ecosystem fluxes of matter and energy can be influenced by variation in climate and vegetation phenology.

For example, Buermann et al. (2001) showed that incorporation of realistic, not prescribed, leaf area index (LAI) helped to eliminate a known cold bias in the US National Center for Atmospheric Research (NCAR) Community Climate Model version 3 (CCM3). Bonan et al. (2002) showed that incorporation of spatially variable LAI strongly affected sensible versus latent heat partitioning in climate modeling. Variations in large-area LAI (Myneni et al., 1997a; Zhou et al., 2001), primarily controlled by temperature changes (Zhou et al., 2003), thus have the potential to strongly alter terrestrial

Received 30 November 2003. Accepted 1 April 2004.

M.A. White.[1] Department of Aquatic, Watershed, and Earth Resources, Utah State University, 5210 Old Main Hill, Logan, UT 84322-5210, USA.

R.R. Nemani. NASA Ames Research Center, Moffett Field, CA 94035, USA.

[1]Corresponding author (e-mail: mikew@cc.usu.edu).

© 2004 CASI

ecosystem processes. Other authors have shown the effect of precipitation (Nemani et al., 2002) and temperature (Braswell et al., 1997) on terrestrial ecosystems.

Numerous authors have investigated aspects of the relationships among climate, LAI, and ecosystem function, e.g., Lucht et al. (2002). To date, many researchers have focused on long-term processes and trends. Although information is becoming available on shorter term controls of ecosystem processes, especially carbon (Baldocchi et al., 2001), the emerging field of short- to long-term ecological and (or) ecosystem forecasting is less understood.

Ecological forecasts, in which the state of an ecosystem is predicted at some time in the future, are of major interest to a wide political and management field. Some ecological forecast applications, such as fire, are especially relevant (Westerling et al., 2002), but fields as diverse as famine relief, agricultural irrigation, power generation, wildlife management, and futures trading could all benefit from ecological forecasts, especially with regard to water resources. In the field of fire control, short-term forecasts could be used to optimize the scheduling of finite resources and (or) request additional support. Various approaches have been used to forecast some portion of the hydrologic cycle, e.g., El Niño – Southern Oscillation (ENSO) teleconnections and streamflow (Chiew et al., 2003), numerical modeling for flood management (Paudyal, 2002), and probabilistic drought forecasts (Anderson et al., 2000). Hydrological forecasts within a larger ecological context, though, are less common.

The terrestrial observation and prediction system (TOPS, http://www.ntsg.umt.edu/tops/) described in Nemani et al. (2003c) and used in Nemani et al. (2003a) can be used to generate such forecasts, including simulation of net primary production (NPP), water fluxes, and soil water content. Prior to implementation in any management application, an understanding of the factors controlling ecological forecasts and the likely impact of errors in forecasts of critical driving variables is required. Our first goal in this research was therefore to assess the relative importance of the time-dependent TOPS input variables, LAI and meteorology, for simulations of soil water content, a critical state variable for many applications. Based on these results, our second goal was to establish the forecast errors in the more important TOPS input variable that would lead to statistically significant differences in forecasted soil water content. Given that TOPS incorporates soil water processes, canopy fluxes, radiation interception, and remote sensing concepts that are in wide use by many modeling groups, we expect our results to be generally applicable to an extensive scientific and management community

Methods

Model

We used TOPS to simulate 1982–1997 (1994 not simulated owing to satellite failure) daily soil water ($kg \cdot m^{-2}$). TOPS integrates remote sensing, ecosystem modeling, and static edaphic and land cover information to simulate ecosystem states and processes. TOPS is derived from the Biome-BGC model (Thornton et al., 2002; White et al., 2000), which in turn is based on the Forest-BGC model (Running and Coughlan, 1988; Running and Gower, 1991). The full Biome-BGC model simulates states and fluxes of ecosystem carbon, nitrogen, and water with prognostic phenology (White et al., 1997), mass and energy balance, and considerations of atmospheric and structural disturbances; TOPS implements the Biome-BGC water flux model, based on a Penman–Monteith approach relying on LAI and meteorology. Daily water fluxes are evapotranspiration (ET), calculated as the sum of transpiration, soil evaporation, canopy evaporation, and sublimation; and runoff, calculated as soil water in excess of soil water holding capacity (calculated from equations in Clapp and Hornberger (1978)). Soil water content, which in turn affects leaf water potential and stomatal conductance, is the balance between inputs (snowmelt and precipitation) and outputs (ET and runoff, calculated using a bucket model). Biome-BGC carbon and nitrogen processes are not used. Instead, consistent with application of TOPS for real-time and forecast modes, carbon fluxes are calculated based on a light-use efficiency model:

$$\text{productivity} = \varepsilon \times \text{APAR} \times f(\text{environment})$$

where ε is the dry matter conversion efficiency (constant of 1.2 $g \cdot MJ^{-1}$ for all biomes, consistent with Green et al. (2003)); f(environment) is a multiplier set as the minimum of limitations from leaf water potential, night minimum temperatures, and vapor-pressure deficit (each is a zero to one scalar, also used for water fluxes); and APAR is absorbed photosynthetically active radiation, calculated as photosynthetically active radiation (PAR) multiplied by the fraction of photosynthetically active radiation (FPAR) absorbed by plant canopies (Myneni et al., 1997b). Nemani et al. (2003a) used TOPS to simulate historical NPP, but here we adopt the premise that soil water, which controls leaf water potential and runoff, is of broadest interest for the management community.

Datasets and processing

As described later in the paper, TOPS simulations require two basic input types: static (soils, land cover) and dynamic (LAI, meteorology). Simulation spatiotemporal resolution was constrained by satellite and meteorological data availability. Both are available for the conterminous US at a resolution of 1 km: satellite data from the Earth Resources Observation System Data Center from 1989 to present and meteorology data from the Daymet project from 1982 to 1997. Satellite data are available from the Pathfinder project from 1982 to present at a resolution of 8 km. As 1 km resolution data overlapped for only the 1989–1997 period, we opted for the longer record of the Pathfinder data and conducted all simulations at a resolution of 8 km for 1982–1997 (Daymet data through 1997 only, 1994 excepted owing to satellite failure). All data were, if necessary, extracted from their full extent, resampled to the 8 km

 © 2004 CASI

resolution, and projected to the Lambert azimuthal equal-area projection.

Static information

Using a 1 km gridded soils dataset from the Pennsylvania State University (based on State Soil Geographic Database, STATSGO, and created by Miller and White (1998)), we generated soil depth and percent sand, silt, and clay, as required by TOPS. For each 1 km pixel, the input data consisted of 11 soil layers, each for a prescribed depth in centimetres (5, 10, 20, 30, 40, 60, 80, 100, 150, 200, and 250), rock fraction, percent sand, silt, and clay, and texture (i.e., silty loam). Depth to bedrock was also included. Thus depth could be obtained from either depth to bedrock or by examining the 11 layers. In many cases the two depths did not agree, even to a coarse approximation. Further, many cases existed in which soil texture was present but sand, silt, and clay data were missing. Other pixels existed with depth information but no other data. Unfortunately, no clear-cut approach for generating single-layer percent sand, silt, and clay and depth existed. We used the following process. First, for each pixel, we extracted only those layers having a depth less than or equal to the recorded depth to bedrock. Second, for these layers we then extracted, where available, the sand, silt, clay, and texture information. Third, we calculated the layer-weighted percent sand, silt, and clay information. Fourth, we calculated the rock fraction corrected layer-weighted soil depth. The 1 km data, although a great improvement over previous datasets, is problematic. Inconsistent or incomplete data are common and uncertainties are largely unknown. Alternatives were extremely limited and we used the dataset with the recognition that it may cause unrealistic simulations in at least some regions (i.e., the Mississippi delta region had a high rock fraction).

Although Lathrop et al. (1995) found that STATSGO data can cause errors in prediction of soil water holding capacity and subsequent simulation of ecosystem processes, Juracek and Wolock (2002) showed that errors are reduced with increasing pixel size, in their case 25 km^2. Thus, as our pixels are 64 km^2 and our results are presented primarily at an aggregate biome level, potential soil-related biases that could hamper fine-resolution studies are not relevant here.

TOPS, in general, is designed for coarsely defined plant functional types as parameterized in White et al. (2000). Here, as our primary goals were to test relative ecosystem forcing by meteorology versus LAI and the system response to input variable forecast errors, we implemented a further biome simplification to four biomes (described in **Figure 1**): deciduous broadleaf forest (DBF), evergreen needle-leaf forest (ENF), grass, and shrub. We identified simulation cells as those containing both valid soils and land cover information (barren and water classes also excluded).

LAI

We used 1982–1997 10-day composited global 8 km Pathfinder advanced very high resolution radiometer (AVHRR) normalized difference vegetation index (NDVI) recomposited to monthly resolution to calculate LAI (and FPAR, not presented) using methods in Myneni et al. (1997b). Although they do not explicitly detect the initiation or completion of plant growth or other ecosystem processes, these data depict the interannual variation and any trends in vegetation phenology. We implemented the following six-step scheme to generate daily LAI values for each pixel. First, we assumed that monthly composited data did not require cloud screening, as is required with shorter term compositing (White et al., 2002). Although unlikely to be true (see later in the paper), this assumption, given the difficulties in accurately cloud-screening historical AVHRR data, was acceptable. Second, we assumed that each composit period represented the midpoint of each month. Third, we calculated the 15-year average for each month (1994 and any missing values not included). Fourth, for each year we identified missing values or LAI calculated as zero and filled these periods with the climatological LAI values from step three. Throughout the spring, summer, and fall months, LAI filling was required in less than 1% of pixels; the maximum filling was 13% for grass biome in January (**Table 1**). Fifth, as extensive analysis revealed considerable residual temporal irregularities, most likely related to partial cloud or snow cover, we applied a three-period smoothing function. Lastly, we used a spline function to generate daily LAI values. These steps yielded, for each pixel, a 15-year time series of daily LAI.

Meteorology

We used 1 km meteorological surfaces generated from the Daymet algorithm (Thornton et al., 1997) using daily weather station observations of maximum–minimum temperatures and precipitation. Daily weather surfaces, generated with recent interpolation improvements (Thornton and Running, 1999; Thornton et al., 2000), include maximum–minimum temperature, short-wave radiation (from which PAR may be calculated), vapor-pressure deficit, and precipitation. Details and data are available on the Daymet Web site (www.daymet.org).

Simulations and analysis: relative forcing

Using these data and the TOPS architecture, we first conducted a 1982–1997 spin-up simulation to initialize system state variables and then conducted the following three simulations:

(1) Control simulation — Both LAI and meteorology were allowed to vary realistically.

(2) Climatological meteorology/variable LAI (CMVL) simulation — For CMVL, we set LAI as for the control simulation. We set maximum–minimum temperatures, radiation, and vapor-pressure deficit as daily 1982–1997 averages, i.e., for each pixel, each day in the climatological meteorology record was a 15-year average. For precipitation, simple averaging was inappropriate, as this would have caused a constant drizzle. Instead, for

© 2004 CASI

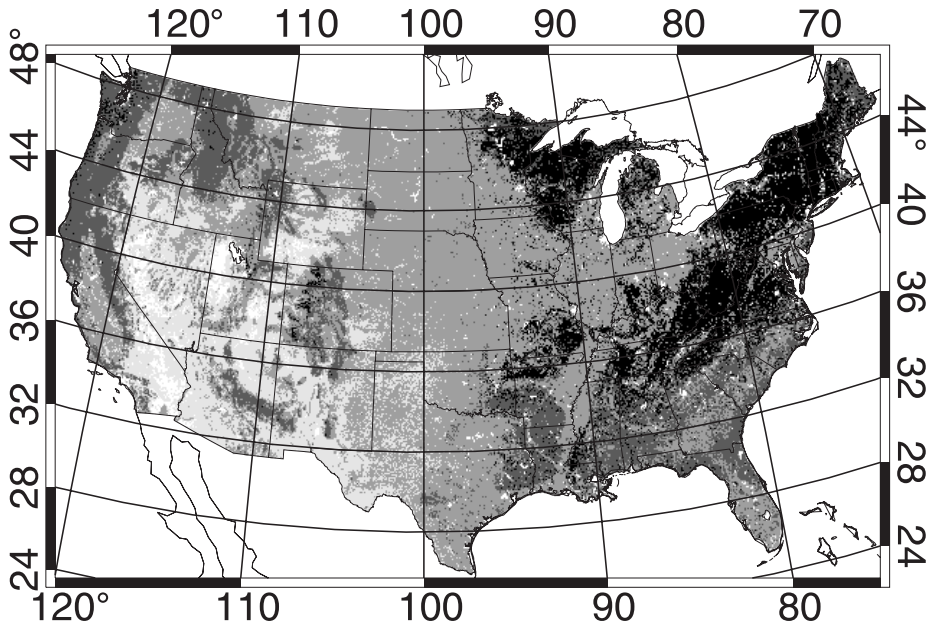

	pixels	1980–1997 mean annual temperature (°C) mean	σ	1980–1997 mean annual total precipitation (cm) mean	σ
DBF	15 422	9.8	4.1	116.9	27.0
ENF	24 094	10.8	6.3	116.0	46.2
Grass	58 438	11.4	5.0	74.6	35.5
Shrub	18 258	12.3	4.8	34.1	14.7

Figure 1. Distribution of biomes used in the TOPS simulations. Land cover data were derived from a combination of the University of Maryland (UMD) classification of Hansen et al. (2000) and the continuous fields classification of DeFries et al. (1999). Deciduous broadleaf forest (DBF) includes mixed forest if evergreen cover less than 50%; woodland if evergreen cover less than 50% and broadleaf cover greater than 50%; wooded grassland if tree cover greater than 50%, evergreen cover less than 50%, and broadleaf cover greater than 50%; and urban. Evergreen needle leaf forest (ENF) includes mixed forest if evergreen cover greater than 50% or broadleaf less than 50%; woodland if evergreen cover greater than 50% or broadleaf cover less than 50%; and wooded grassland if tree cover greater than 50% and evergreen cover greater than 50% or broadleaf cover less than 50%. Grass includes grassland; wooded grassland if tree cover less than 50%; and cropland. Shrub includes closed and open shrub.

each month and each pixel, we calculated average total precipitation and average number of days with rain. Precipitation was then randomly distributed within the month based on these data. CMVL simulations thus show the impact of ignoring realistic interannual climatic variability.

(3) Climatological LAI and variable meteorology (CLVM) simulation — Here, for each pixel, we set daily LAI as the corresponding 1982–1997 daily average LAI and daily weather as for the control simulation. CLVM simulations thus show the impact of replacing realistic interannual LAI – phenological variability with long-term average canopy seasonality. Note that this scenario does not employ the same LAI value for every day in the year: the long-term average seasonality is present.

We then conducted a three-step analysis, each of which, by examining the divergence of CMVL–CLVM from the control simulation, indicates the relative importance of meteorology versus LAI in forcing simulated soil water.

We first assessed the differences in soil water content by season: January, February, March (JFM); April, May, June (AMJ); July, August, September (JAS); and October, November, December (OND). For each season in each year we extracted the simulated daily soil water and conducted a *t* test between the approximately 90 days in the experimental (CMVL or CLVM) and control simulations. We recorded the

© 2004 CASI

Table 1. Percentage of LAI values filled with climatological values.

	DBF	ENF	Grass	Shrub
January	4	3	13	9
February	3	2	8	5
March	1	1	2	1
April	0	0	0	0
May	0	0	0	0
June	0	0	0	0
July	0	0	0	0
August	0	0	0	0
September	0	0	0	0
October	0	0	0	0
November	1	1	2	1
December	3	3	10	6

Note: Zero indicates less than 0.5%. DBF, deciduous broadleaf forest; ENF, evergreen needle-leaf forest.

number of years (out of a potential 15) with a probability value P less than 0.05. For each biome, we also calculated the percentage of annual simulations with significant differences in each season.

Second, we investigated the relationship among annual meteorology, LAI, and the number of significant differences between CMVL–CLVM and control simulations. For meteorology, we used annual average water deficit, equal to the control precipitation minus control potential ET (calculated using a Priestley–Taylor approach), which integrates the influence of moisture inputs, radiation, temperature, and humidity. Preliminary results showed that patterns were generally consistent among seasons, and we therefore compressed the analysis to show the total number of significant differences (maximum of 60, or 15 years and four seasons) in relation to pixel water deficit and LAI. Essentially, we here sought to assess whether or not persistent significant differences between the experimental (CMVL–CLVM) and control simulations were related to patterns in meteorology or LAI.

Third, we conducted a wavelet analysis of daily, biome-averaged soil water differences between the control and experimental (CMVL–CLVM) simulations. Wavelet transformations (Csillag and Kabos, 2002) are similar to Fourier transformations but instead rely on the translation and dilation of a wavelet function such that the function is nonzero for a finite distance. Consequently, wavelet analysis can show the extent to which the signal or image matches the wavelet function at particular locations and resolutions. In an excellent and comprehensible guide to wavelets, Torrence and Compo (1998) showed how wavelet analysis could be used to determine the structure and timing of ENSO. Using their methods and a Morlet wavelet function with wavenumber equal to six, we calculated the nonorthogonal continuous wavelet power spectrum (equal to the square of the absolute value of the wavelet amplitude). Conceptually, the wavelet power spectrum shows how the input signal (difference between control and experimental simulations) corresponds to the wavelet function at a particular translation (1982–1997) and dilation (1 day to several years).

Simulations and analysis: meteorological forecast errors

Simulations from the previous analysis indicated that meteorology was the dominant forcing factor of simulated soil water at both pixel and biome levels (see Results). Based on this information, we next identified the meteorological forecast error required to induce a statistically significant biome-level difference at the end of a 7-day soil water forecast. The 7-day forecast time is somewhat arbitrary but is a relevant time scale for many management decisions.

For each biome, we considered the effects of four meteorological forecast errors: (*i*) hot and wet (HW), (*ii*) hot and dry (HD), (*iii*) cold and wet (CW), and (*iv*) cold and dry (CD). To generate the forecast errors, we first calculated the standard deviation of 1982–1997 daily maximum and minimum temperatures. Using this information, we induced progressively more extreme meteorological forecast errors (see **Figure 2** for schematic). We set the initial forecast error at 0.1 (–0.1) standard deviations (σ) for temperature and 5% (–5%) for precipitation for hot (cold) and wet (dry) scenarios. For example, the initial HW forecast error would include an increase in maximum and minimum temperature of 0.1 standard deviations and a 5% increase in precipitation for all days from 1 to 7 January. We did not vary radiation or humidity fields. We then simulated soil water for the same time period using the true Daymet meteorology. Next, we compared soil water simulated with the true and erroneous meteorology at the end of the 7-day period (7 January for the first week). If a t test showed significant differences at the 5% level between the simulations using the altered and original meteorology, we

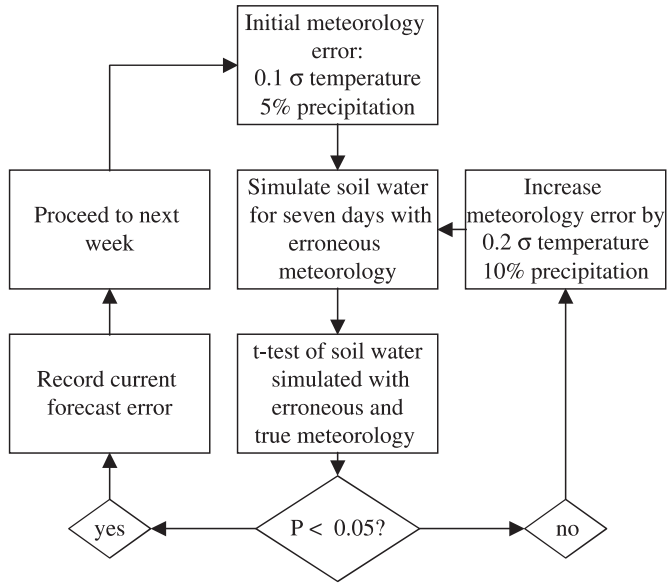

Figure 2. Procedure for identifying the meteorological forecast error producing a statistically significant difference in biome-level soil water at the end of a 1-week forecast. This procedure was conducted from 1982 to 1997 for 50 weeks per year in all biomes.

© 2004 CASI

recorded this meteorological forecast critical error. If not, we increased the alteration of the meteorological forecast by increments of 0.2 standard deviations for temperature and 10% for precipitation. Meteorological forecast errors were iteratively increased until either significantly different soil water was reached or a maximum perturbation of 2.1 standard deviation increase (decrease) in temperature and a 105% (–95%) change in precipitation was reached.

We conducted the same exercise for 50 weeks, each beginning 7 days apart (i.e., 1 January, 8 January, etc.), and for all years from 1982 to 1997. Simulations thus depicted, for each biome and each meteorological forecast scenario, the seasonally variable meteorological forecast error required to induce statistically different biome-level soil water forecasts. Note that no ordinal relationship is implied: the differences could be positive or negative.

Results

Relative forcing

Interannual variability in meteorology exerted a stronger control over simulated seasonal soil water than did interannual variability in LAI (**Figure 3**). Holding meteorology to its climatological values in the CMVL scenario produced persistent differences in soil water, especially in the interior west. Compared with other areas within the west, mountainous and coastal regions tended to have fewer years with significant differences. The east, especially in JFM and OND, had many fewer years with significant differences. JAS, though, exhibited a high number of impacted years in the east. The northern regions of the east, such as New England and Minnesota, demonstrated patterns opposite to those of the rest of the east in JFM and OND. In the CMVL versus control comparison, the shrub biome was most sensitive and had at least 85% of pixel years impacted (**Table 1**). Biome impacts were next highest for grass, with ENF approximately equal to DBF (**Table 2**). In the CMVL scenario, only DBF in JFM and OND and ENF in JFM had less than 50% of simulations affected.

By comparison, the CLVM scenario exhibited minor divergence from the control scenario (**Figure 3**). In all seasons, much of the eastern United States had no years with significant differences, i.e., the CLVM scenario was statistically similar to the control. Again, larger impacts occurred in the west, with a clear division running northward from central Texas. Maximal effects occurred in the northern Great Plains in JFM and OND and in the desert southwest in all seasons. The west coast rarely had any significant differences. By biome, ordinal relationships were similar to those of the CMVL scenario, with shrub > grass > ENF > DBF (**Table 2**). The magnitude in CLVM, though, was smaller than that in CMVL, and no biome had more than 50% of simulations with significant differences. In all seasons in the DBF and ENF biomes, less than 10% of simulations were affected (**Table 2**).

As suggested by spatial patterns in **Figure 3**, the number of simulations with significant differences between control and experimental (CMVL–CLVM) scenarios was related to climate and LAI (**Figure 4**). For both CMVL and CLVM, increases in the number of affected simulations were strongly associated with declines in water deficit and LAI. In other words, a pixel with very frequent differences between the control and either experimental scenario was likely to have a large water deficit and low average LAI.

The wavelet analysis again shows that climatic variation was more important than LAI variation for simulation of soil water (**Figure 5**). The wavelet power spectra (upper portion of panels) illustrate that, when viewed at a biome level, CMVL (**Figures 5a–5d**) induced extensive differences in soil water at multiple scales and at many signal translations throughout 1982–1997. CLVM did not. ENF (**Figure 5a**) and DBF (**Figure 5b**) had strong signals at 1-year and multiyear (1000–1500 days) scales, with peak spectra from 1982 to 1992. For grass (**Figure 5c**) and shrub (**Figure 5d**), the annual scale was less prominent but the multiyear scale produced even higher spectra. The CLVM wavelet power spectrum (**Figures 5e–5h**), when shown on the same color scale as CMVL, was practically absent, except for very low spectra in grass (**Figure 5g**) and shrub (**Figure 5h**).

The lower portion of each panel, showing the difference in daily biome-level soil water between the control and experimental (CMVL–CLVM) simulations, further supports the argument that meteorology variation impacted soil water simulation more strongly than LAI variation. In addition to the larger absolute magnitudes of the differences in CMVL than in CLVM, several other patterns are apparent: (*i*) for grass and shrub, most of the differences were greater than zero, indicating that the control simulations generated higher soil water than CMVL; (*ii*) for all biomes, differences were low or negative in the late 1980s and high in the early 1980s and late 1990s; and (*iii*) trends in the differences existed, especially from the late 1980s to the end of the record.

Meteorological forecast errors

In 13 out of a potential 16 biome–season combinations, the seasonal temperature critical error exhibited a U shape or inverted U shape (**Figure 6**). Weeks 15–35 (approximately mid-April to early September) were susceptible to temperature forecast errors of ±2.5 °C in nearly all scenarios. Critical errors in winter approached ±10 °C, indicating that extremely erroneous temperature forecasts were required to induce significant errors in simulated 1-week soil water forecasts. Although most scenarios had similar temperature critical errors in summer, HW remained more sensitive to errors in the winter than did HD, CW, or CD. Although shrub and ENF tended to show a flattened annual curve, most biomes varied surprisingly little in the shape of their temperature critical errors. Variability in the temperature critical error tended to be lowest in summer and highest in winter.

In comparison to temperature, the precipitation critical error was much more consistent throughout the year (**Figure 7**). DBF and ENF biomes in HD and CW scenarios had the U shape

 © 2004 CASI

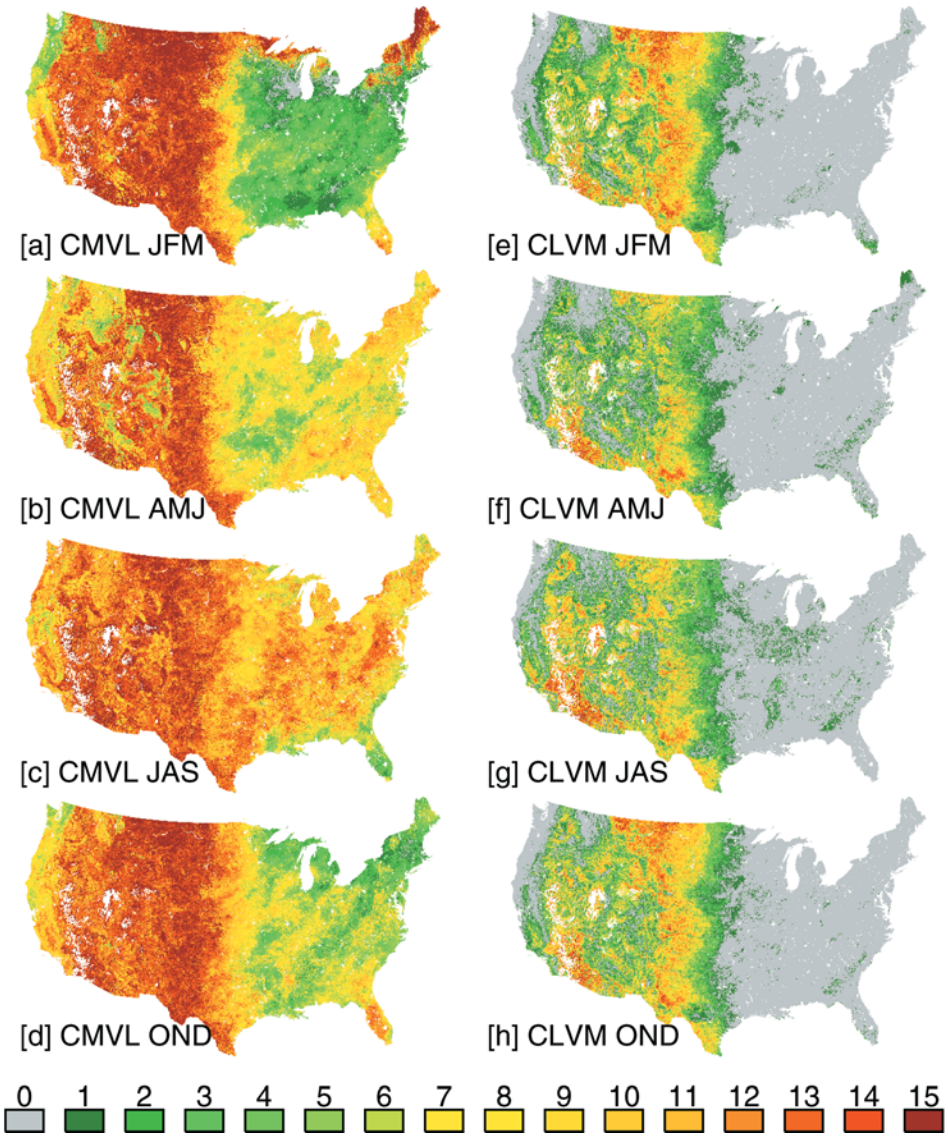

Figure 3. Number of years (1–15) with statistically significant (5% level) differences in seasonal soil water between experimental and control simulations. Experimental simulations are either climatological meteorology variable LAI (CMVL) or climatological LAI variable meteorology (CLVM). Seasons are January, February, and March (JFM); April, May, and June (AMJ); July, August, and September (JAS); and October, November, and December (OND).

Table 2. Percentage of 1982–1997 seasonal soil water simulations with statistically significant differences between experimental and control simulations.

	DBF		ENF		Grass		Shrub	
	CMVL	CLVM	CMVL	CLVM	CMVL	CLVM	CMVL	CLVM
JFM	35	1	48	6	62	24	91	47
AMJ	56	0	52	2	67	14	85	38
JAS	71	0	63	5	79	18	89	48
OND	34	0	51	6	71	24	88	46

Note: AMJ, April, May, and June; CLVM, climatological LAI variable meteorology; CMVL, climatological meteorology variable LAI; JAS, July, August, and September; JFM, January, February, and March; OND, October, November, and December.

© 2004 CASI

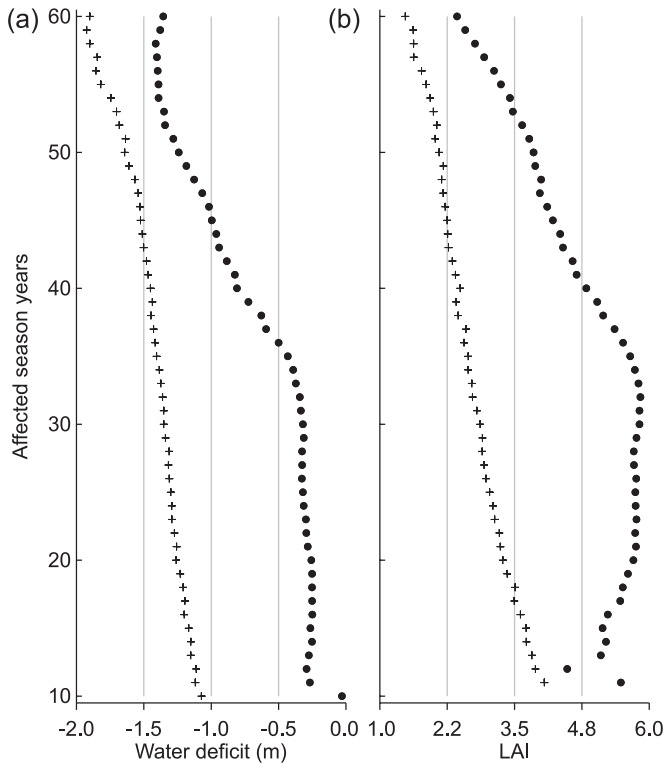

Figure 4. Relationship between the number of affected simulations and (a) water deficit and (b) LAI. This figure is based on a combination of separate seasonal analysis, most of which showed highly similar patterns. The *y* axis shows the number of simulations with statistically different soil water content (at the 5% level). Note that each point does not show the number of pixels in each bin, simply the relationship between affected simulations years (maximum of 60:15 years and four seasons) and explanatory variables (average annual water deficit and LAI). Simulations show CMVL versus control (solid circles) and CLVM versus control (crosses). The number of pixels in bins of affected simulations varies greatly between CMVL and CLVM, creating the perception of differences in the absolute magnitude of explanatory variables; both are derived from the same input data and have identical mean water deficit and LAI. Data are for the entire simulation area and do not distinguish among biomes.

common in **Figure 6** and a large variability in the winter precipitation critical error. The remainder of biome–season combinations did not; most had low variability throughout the year and a critical error of less than 1 cm for total 1-week precipitation.

Discussion

Relative forcing

Our exploration of the relative forcing of ecosystem soil water suggests that climatic variation is a stronger influence than LAI (**Figures 3–5**). For limited durations, mostly in the shrub and grass biomes, interannual phenological variability was important (**Figure 3**), but in general, ignoring interannual LAI variation appears to have a relatively minor impact on soil water forecasts. We were somewhat surprised by this finding, given the documented importance of vegetation phenology in a wide global change community (Menzel, 2002; Parmesan and Yohe, 2003) on climate and weather (Lu and Shuttleworth, 2002; Schwartz, 1992; Schwartz and Crawford, 2001; Xue et al., 1996), on vegetation distribution (Chuine and Beaubien, 2001), and, depending on definitions used, on the terrestrial carbon cycle (Baldocchi et al., 2001; Keeling et al., 1996; Randerson et al., 1999; White et al., 1999; White and Nemani, 2003). We believe that at least three factors may affect the importance of LAI on simulated soil water in this study.

First, the coarse time resolution (monthly) of the input AVHRR data may have removed fine differences in interannual LAI variability. The alternate 10-day data would have generated extremely spurious results due to nonvegetative (i.e., contaminated) LAI irregularities. Regardless, extensive interannual LAI variability was still present in the monthly data and use of a finer time resolution would not have induced significantly different results. Second, poor radiometric resolution of the AVHRR inevitably limited the accuracy of results. Third, the CLVM simulations were forced by the realistic, long-term phenological signal: LAI was not the same every day. In CLVM, 1 January would have had the same value for 1982–1997, but LAI from 1 January to 31 December would have varied, following the 1982–1997 average seasonality. Thus the main forcing from the average phenological signal was still present in CLVM, with only the interannual variability removed. These simulations therefore must not be interpreted to imply that vegetation seasonality or systematic biases in remotely sensed LAI have no effect on simulated soil water, only that interannual LAI variations were less important than interannual climatic variation. In a global study using two independently processed remote sensing datasets, Nemani et al. (2003b) found similar results for NPP simulations.

Figures 3 and **4** suggest that, in both the CMVL and CLVM scenarios, persistently effected regions had low annual precipitation and low LAI. Similarly, Guillevic et al. (2002) found that in global simulations of evapotranspiration, sparsely vegetated regions, especially when wet, were highly sensitive to remotely sensed vegetation variability. Guillevic et al. also stated that "Although interannual variations in vegetation properties still influence transpiration and interception loss at the global scale in these runs, their impact on large-scale regional climate is much weaker, apparently because the impact is drowned out by atmospheric variability." Our findings, with a different modeling approach, examination of soil water not water fluxes, a finer spatial resolution, and a longer temporal record, also suggest that atmospheric variability exerts a dominant control over interannual vegetation variability.

Meteorological forecast errors

Figures 6 and **7** provide a quantitative estimate of the meteorological forecasts that will generate statistically different 1-week soil water forecasts for the biomes shown in **Figure 1**. These simulations have some limitations. First,

© 2004 CASI

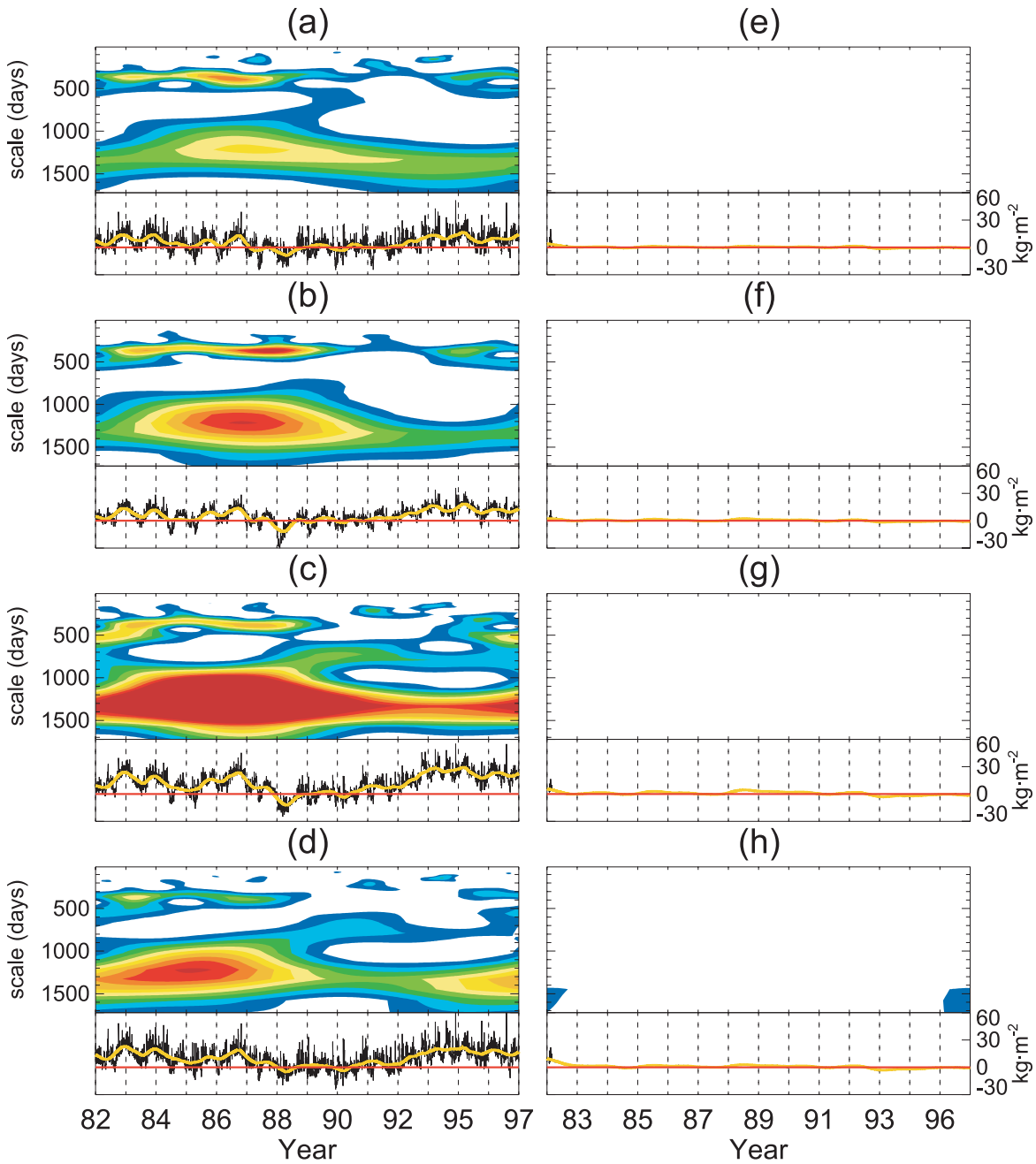

Figure 5. Wavelet analysis of 1982–1997 daily differences in biome-averaged soil water between (a–d) climatological meteorology variable LAI (CMVL) and control and (e–h) climatological LAI variable meteorology (CLVM) and control. The biomes shown in **Figure 1** are represented by panels a and e (ENF), b and f (DBF), c and g (grass), and d and h (shrub). The upper portion in each panel shows the continuous wavelet transformation wavelet power spectrum (square of the absolute value of the wavelet amplitude) ranging from low (blue) to high (red–brown) at length scales ranging from 1 to 1825 days. CLVM power spectra are present but are usually so much lower than in CMVL that they do not appear in the color scheme. Lower panels show the differences in $kg \cdot m^{-2}$. The red horizontal line is zero difference, and the yellow line is the daily signal convolved with a Savitzky–Golay filter with a 1-year width.

agricultural regions are treated as grass: the results for these regions therefore cannot be used for crop management or forecasting. TOPS does employ an irrigation mechanism by which soil water potential is maintained at a user-specified level but, given the considerable variability in crop variety and management and the relatively coarse spatial resolution of these simulations, we chose not to simulate agricultural areas. At a finer resolution and with detailed crop information, TOPS can be used in agricultural applications (Nemani et al., 2003c). Second, the information is presented at a biome level. Smaller

© 2004 CASI

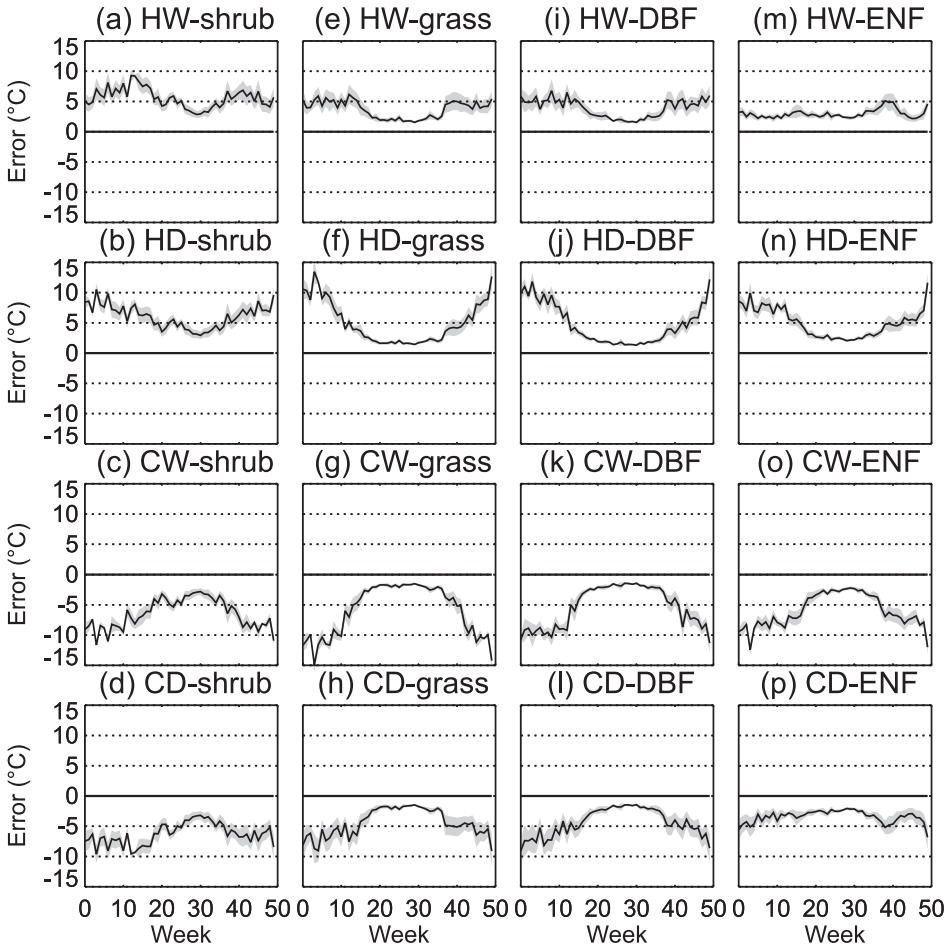

Figure 6. Temperature critical errors by biome and season. The *x* axes show time in weeks from 0 (early January) to 50 (late December), and the *y* axes show the biome-averaged meteorological forecast error (1-week average temperature) required to generate statistically significant differences (5% level) in biome-level soil water. Shaded portions show the standard deviation of the 1982–1997 average. Panel rows are organized by meteorological forecast error type, namely hot and wet (HW), hot and dry (HD), cold and wet (CW), and cold and dry (CD), and the panel columns by biome shown in **Figure 1**, namely ENF, DBF, grass, and shrub. See text for description of simulation process.

regions may have different sensitivities to meteorological forecasts. Given the relatively consistent shape of many of the seasonal critical errors, though, we feel that the findings are robust. Third, the simulations do not show ordinal information. For many management applications, errors in one direction may be the only concern. Fourth, we present data for 1-week soil water forecasts. For long-lead management projects, such as famine relief, this information may not be useful.

We found that temperature critical errors were relatively unimportant in colder seasons, probably owing to lower evaporative potential in cold, low-radiation periods. Essentially, irrespective of the error in precipitation, winter temperature errors had little effect on soil water forecasts.

Although precipitation critical errors were fairly constant, some unexpected interactions occurred, especially in the more mesic DBF and ENF biomes. Here for HD and CW, large precipitation errors were required to induce soil water errors. In HD in winter, the higher temperatures increased snowmelt and more precipitation fell as rain, leading to an increase in soil water, even though less precipitation occurred. In essence, the liquid form of H_2O increased with higher winter temperatures; a very large decrease in precipitation input was therefore required to generate a critical error. In CW, the increased input of precipitation was stored more in solid form, leading to a net decrease in soil water, even though inputs increased. Both of these responses, though, had high standard deviation, indicating that the balance between precipitation inputs and the form of storage was spatially and temporally variable.

Variation in time scale sensitivity and potential teleconnections

Wavelet analysis (**Figure 5**) suggests that biomes respond to input forcings at different time scales. The annual scale is strongest in the wavelet power spectrum for DBF and ENF,

 © 2004 CASI

which maintain a generally high LAI in mesic environments. For these biomes, the difference in soil water content between an average meteorological year and an actual wet or dry year is thus magnified by a greater difference in the absolute magnitude of precipitation inputs and a larger canopy with which to process water fluxes.

We speculate that the wavelet power at an approximately 4-year scale is related to ENSO teleconnections. Torrence and Compo (1998) showed ENSO wavelet power was strong at the 4-year scale during the mid- to late 1980s but was low thereafter; **Figure 5** shows the exact same pattern, but with obvious biome-level differences in wavelet power. Scale-averaged wavelet power in the meteorological variables at subannual time scales (not shown but available on request) may provide some explanation for this phenomenon. Three events of high meteorological wavelet power (1984 temperature and precipitation, 1986 precipitation, and 1990 temperature and precipitation) bracket the generally strong 4-year wavelet power signals in **Figure 5**. However, the grass biome had high precipitation wavelet power throughout much of the late 1980s, while the other biomes had average power for most of this period. Haddad et al. (2002) found that grasslands demonstrate a lagged multiyear periodicity in ecosystem processes in response to precipitation cycles; combined with the wavelet signal (**Figure 5c**), this implies that grasslands may have responded more strongly than other biomes did to the ENSO patterns in the 1980s.

Scientific and social issues for ecological forecasting

As regions with low LAI and precipitation are often characterized by pressing societal needs for competent water management decisions, our simulations highlight the crucial nature of improvements in two fields: forecasting and monitoring of precipitation in arid regions, which are often highly heterogeneous (Comrie and Broyles, 2002); and remote sensing of LAI, which is often confounded by soils with variable brightness and wetness (Bannari et al., 1996). In essence, **Figures 3–5** imply that many areas with a potential for high societal benefits from accurate soil water forecasts may also be most strongly affected by errors in input meteorology and (or) LAI. All possible efforts should be made to incorporate the best possible meteorological forecasts into ecosystem forecasting, including research into geographic and seasonal forecast biases.

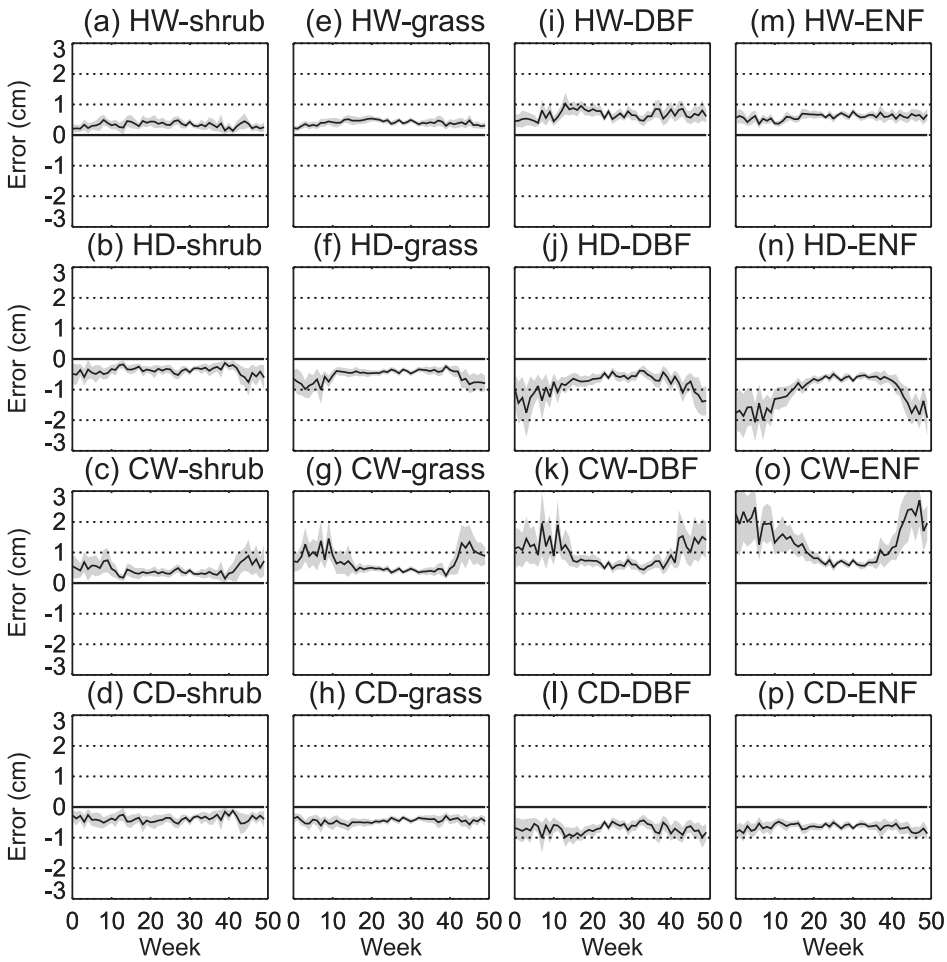

Figure 7. Precipitation critical errors by biome and season. Panels as in **Figure 7**, except the *y* axes show the 1-week total precipitation forecast error.

© 2004 CASI

The importance of understanding forecast errors is well known (Brown, 2002; Changnon and Vonnahme, 2003), as are some of the challenges in implementing forecasts in the management community (Callahan et al., 1999; Pagano et al., 2001). Thus, information on critical errors (**Figures 6** and **7**) is relevant for management uncertainty assessment and planning only in combination with an understanding of actual meteorological forecast errors. Constant updates to forecast models suggest that historical literature assessments of meteorological forecast errors may not be indicative of current model performance; instead, internet-based tools should be used. Near-past assessments of numerous forecast models, at multiple forecast lengths, are available at the National Oceanic and Atmospheric Administration (NOAA) National Weather Service National Center for Environmental Prediction Hydrometeorological Predictions Center (NWS NCEP HPC) interactive model bias page (http://www.hpc.ncep.noaa.gov/mdlbias/). Using this tool, users can relate the performance of meteorological models to forecast sensitivity (**Figures 6** and **7**) to assess, in a real-time sense, the likelihood of significantly erroneous ecological forecasts. Current bias estimates are better for temperature than for precipitation, suggesting that forecasting of variables most strongly affected by temperature, such as phenology or snowmelt, may be highly successful.

The simulations shown here imply that forecasts of soil water are highly dependent on summer temperature forecasts, precipitation forecasts throughout the year, and, to a lesser extent, LAI forecasts in arid regions. We feel that with current technologies, TOPS can be used with a high degree of confidence when ongoing meteorological forecast bias is closely tracked and interpreted in the context of **Figures 6** and **7**. With continual improvements in meteorological forecasting technology and remote sensing, we expect that TOPS will become a consistently useful tool for the arid regions most critically in need of soil water content management.

Acknowledgments

M.A. White was supported by National Aeronautics and Space Administration (NASA) grant NAG5-11282 and National Science Foundation (NSF) grant GEO-0222701, and R. Nemani by grants from the NASA Earth Science Enterprise (ESE) and Computing, Information and Communications Technology (CICT) programs.

References

Anderson, M.L., Mierzwa, M.D., and Kavvas, M.L. 2000. Probabilistic seasonal forecasts of droughts with a simplified coupled hydrologic–atmospheric model for water resources planning. *Stochastic Environmental Research and Risk Assessment*, Vol. 14, pp. 263–274.

Baldocchi, D., Falge, E., and Wilson, K. 2001. A spectral analysis of biosphere–atmosphere trace gas flux densities and meteorological variables across hour to multi-year time scales. *Agricultural and Forest Meteorology*, Vol. 107, pp. 1–27.

Bannari, A., Huete, A.R., Morin, D., and Zagolski, F. 1996. Effects of soil color and brightness on vegetation indexes. *International Journal of Remote Sensing*, Vol. 17, pp. 1885–1906.

Bonan, G.B., Levis, S., Kergoat, L., and Oleson, K.W. 2002. Landscapes as patches of plant functional types: an integrating concept for climate and ecosystem models. *Global Biogeochemical Cycles*, Vol. 16, No. 1021.

Braswell, B.H., Schimel, D.S., Linder, E., and Moore, B.I. 1997. The response of global terrestrial ecosystems to interannual temperature variability. *Science (Washington, D.C.)*, Vol. 278, pp. 870–872.

Brown, K. 2002. Environmental data — water scarcity: Forecasting the future with spotty data. *Science (Washington, D.C.)*, Vol. 297, pp. 926–927.

Buermann, W., Dong, J., Zeng, X., Myneni, R.B., and Dickinson, R.E. 2001. Evaluation of the utility of satellite-based vegetation leaf area index data for climate simulations. *Journal of Climate*, Vol. 14, pp. 3536–3550.

Callahan, B., Miles, E., and Fluharty, D. 1999. Policy implications of climate forecasts for water resources management in the Pacific Northwest. *Policy Sciences*, Vol. 32, pp. 269–293.

Changnon, S.A., and Vonnahme, D.R. 2003. Impact of spring 2000 drought forecasts on Midwestern water management. *Journal of Water Resources Planning and Management, ASCE*, Vol. 129, pp. 18–25.

Chiew, F.H.S., Zhou, S.L., and McMahon, T.A. 2003. Use of seasonal streamflow forecasts in water resources management. *Journal of Hydrology*, Vol. 270, pp. 135–144.

Chuine, I., and Beaubien, E. 2001. Phenology is a major determinant of tree species range. *Ecology Letters*, Vol. 4, No. 5, pp. 500–510.

Clapp, R.B., and Hornberger, G.M. 1978. Empirical equations for some soil hydraulic properties. *Water Resources Research*, Vol. 14, pp. 601–604.

Comrie, A.C., and Broyles, B. 2002. Variability and spatial modeling of fine-scale precipitation data for the Sonoran Desert of southwest Arizona. *Journal of Arid Environments*, Vol. 50, pp. 573–592.

Csillag, F., and Kabos, S. 2002. Wavelets, boundaries, and the spatial analysis of landscape patterns. *Écoscience*, Vol. 9, pp. 177–190.

DeFries, R.S., Townshend, J.R.G., and Hansen, M.C. 1999. Continuous fields of vegetation characteristics at the global scale at 1 km resolution. *Journal of Geophysical Research, Atmospheres*, Vol. 104, pp. 16 911 – 16 923.

DeFries, R.S., Bounoua, L., and Collatz, G.J. 2002. Human modification of the landscape and surface climate in the next fifty years. *Global Change Biology*, Vol. 8, pp. 438–458.

Green, D.S., Erickson, J.E., and Kruger, E.L. 2003. Foliar morphology and canopy nitrogen as predictors of light-use efficiency in terrestrial vegetation. *Agricultural and Forest Meteorology*, Vol. 115, pp. 163–171.

Guillevic, P., Koster, R.D., Suarez, M.J., Bounoua, L., Collatz, G.J., Los, S.O., and Mahanama, S.P.P. 2002. Influence of the interannual variability of vegetation on the surface energy balance — a global sensitivity study. *Journal of Hydrometeorology*, Vol. 3, pp. 617–629.

Haddad, N.M., Tilman, D., and Knops, J.M.H. 2002. Long-term oscillations in grassland productivity induced by drought. *Ecology Letters*, Vol. 5, pp. 110–120.

Hansen, M.C., DeFries, R.S., Townshend, J.R.G., and Sohlberg, R. 2000. Global land cover classification at 1 km resolution using a decision tree classifier. *International Journal of Remote Sensing*, Vol. 21, pp. 1331–1365.

 © 2004 CASI

Imhoff, M., Lawrence, W., Elvidge, C., Paul, T., Levine, E., Privalsky, M., and Brown, V. 1997. Using nighttime DMSP/OLS images of city lights to estimate the impact of urban land use on soil resources in the United States. *Remote Sensing of Environment*, Vol. 59, pp. 105–117.

Juracek, K.E., and Wolock, D.M. 2002. Spatial and statistical differences between 1 : 250 000- and 1 : 24 000-scale digital soil databases. *Journal of Soil and Water Conservation*, Vol. 57, pp. 89–94.

Keeling, C.D., Chin, J.F.S., and Whorf, T.P. 1996. Increased activity of northern vegetation inferred from atmospheric CO_2 measurements. *Nature (London)*, Vol. 382, pp. 146–149.

Lathrop, R.G., Aber, J.D., and Bognar, J.A. 1995. Spatial variability of digital soil maps and its impact on regional ecosystem modeling. *Ecological Modelling*, Vol. 82, pp. 1–10.

Lu, L.X., and Shuttleworth, W.J. 2002. Incorporating NDVI-derived LAI into the climate version of RAMS and its impact on regional climate. *Journal of Hydrometeorology*, Vol. 3, pp. 347–362.

Lucht, W., Prentice, I.C., Myneni, R.B., Sitch, S., Friedlingstein, P., Cramer, W., Bousquet, P., Buermann, W., and Smith, B. 2002. Climatic control of the high-latitude vegetation greening trend and Pinatubo effect. *Science (Washington, D.C.)*, Vol. 296, pp. 1687–1689.

Menzel, A. 2002. Phenology, its importance to the global change community. *Climatic Change*, Vol. 54, pp. 379–385.

Miller, D.A., and White, R.A. 1998. A conterminous United States multilayer soil characteristics dataset for regional climate and hydrology modeling. *Earth Interactions*, Vol. 2, pp. 1–13.

Myneni, R.B., Keeling, C.D., Tucker, C.J., Asrar, G., and Nemani, R.R. 1997a. Increased plant growth in the northern high latitudes from 1981 to 1991. *Nature (London)*, Vol. 386, pp. 698–702.

Myneni, R.B., Nemani, R.R., and Running, S.W. 1997b. Estimation of global leaf area index and absorbed PAR using radiative transfer models. *IEEE Transactions on Geoscience and Remote Sensing*, Vol. 35, pp. 1380–1393.

Nemani, R.R., White, M.A., Thornton, P.E., Nishida, K., Reddy, S., Jenkins, J., and Running, S. 2002. Recent trends in hydrologic balance have enhanced the terrestrial carbon sink in the United States. *Geophysical Research Letters*, Vol. 29, No. 10, Art. No. 1468.

Nemani, R.R., Keeling, C.D., Hashimoto, H., Jolly, W.M., Piper, S.C., Tucker, C.J., Myneni, R.B., and Running, S.W. 2003a. Climate-driven increases in global terrestrial net primary production from 1982 to 1999. *Science (Washington, D.C.)*, Vol. 300, pp. 1560–1563.

Nemani, R.R., Keeling, C.D., Hashimoto, H., Jolly, W.M., Piper, S.C., Tucker, C.J., Myneni, R.B., and Running, S.W. 2003b. Climate-driven increases in global terrestrial net primary production from 1982 to 1999 [online supplementary material]. *Science (Washington, D.C.)*, Vol. 300, pp. 1560–1563.

Nemani, R.R., White, M., Pierce, L., Votava, P., Coughlan, J., and Running, S. 2003c. Biospheric monitoring and ecological forecasting. *Earth Observing Magazine*, Vol. 12, pp. 6–8.

Pagano, T.C., Hartmann, H.C., and Sorooshian, S. 2001. Using climate forecasts for water management: Arizona and the 1997–1998 El Nino. *Journal of the American Water Resources Association*, Vol. 37, pp. 1139–1153.

Parmesan, C., and Yohe, G. 2003. A globally coherent fingerprint of climate change impacts across natural systems. *Nature (London)*, Vol. 421, pp. 37–42.

Paudyal, G.N. 2002. Forecasting and warning of water-related disasters in a complex hydraulic setting — the case of Bangladesh. *Hydrological Sciences Journal*, Vol. 47, pp. S5–S18.

Randerson, J., Field, C., Fung, I., and Tans, P. 1999. Increases in early season ecosystem uptake explain recent changes in the seasonal cycle of atmospheric CO_2 at high northern latitudes. *Geophysical Research Letters*, Vol. 26, pp. 2765–2768.

Running, S.W., and Coughlan, J.C. 1988. A general model of forest ecosystem processes for regional applications. I. Hydrologic balance, canopy gas exchange and primary production processes. *Ecological Modelling*, Vol. 42, pp. 125–154.

Running, S.W., and Gower, S.T. 1991. FOREST-BGC, a general model of forest ecosystem processes for regional applications. II. Dynamic carbon allocation and nitrogen budgets. *Tree Physiology*, Vol. 9, pp. 147–160.

Schwartz, M.D. 1992. Phenology and springtime surface-layer change. *Monthly Weather Review*, Vol. 120, pp. 2570–2578.

Schwartz, M.D., and Crawford, T.M. 2001. Detecting energy balance modifications at the onset of spring. *Physical Geography*, Vol. 22, pp. 394–409.

Thornton, P.E., and Running, S.W. 1999. An improved algorithm for estimating incident daily solar radiation from measurements of temperature, humidity, and precipitation. *Agricultural and Forest Meteorology*, Vol. 93, pp. 211–228.

Thornton, P.E., Running, S.W., and White, M.A. 1997. Generating surfaces of daily meteorological variables over large regions of complex terrain. *Journal of Hydrology*, Vol. 190, pp. 214–251.

Thornton, P.E., Hasenauer, H., and White, M.A. 2000. Simultaneous estimation of daily solar radiation and humidity from observed temperature and precipitation: an application over complex terrain in Austria. *Agricultural and Forest Meteorology*, Vol. 104, pp. 255–271.

Thornton, P., Law, B., Gholz, H., Clark, K., Falge, E., Ellsworth, D., Goldstein, A., Monson, R., Hollinger, D., Paw, U., Chen, J., and Sparks, J. 2002. Modeling and measuring the effects of disturbance history and climate on carbon and water budgets in evergreen needleleaf forests. *Agricultural and Forest Meteorology*, Vol. 113, pp. 185–222.

Torrence, C., and Compo, G.P. 1998. A practical guide to wavelet analysis. *Bulletin of the American Meteorological Society*, Vol. 79, pp. 61–78.

Westerling, A.L., Gershunov, A., Cayan, D.R., and Barnett, T.P. 2002. Long lead statistical forecasts of area burned in western US wildfires by ecosystem province. *International Journal of Wildland Fire*, Vol. 11, pp. 257–266.

White, M.A., and Nemani, R.R. 2003. Canopy duration has little effect on annual carbon storage in the eastern United States broad leaf forest. *Global Change Biology*, Vol. 9, pp. 976–972.

White, M.A., Thornton, P.E., and Running, S.W. 1997. A continental phenology model for monitoring vegetation responses to interannual climatic variability. *Global Biogeochemical Cycles*, Vol. 11, pp. 217–234.

White, M.A., Running, S.W., and Thornton, P.E. 1999. The impact of growing-season length variability on carbon assimilation and evapotranspiration over 88 years in the eastern U.S. deciduous forest. *International Journal of Biometeorology*, Vol. 42, pp. 139–145.

White, M.A., Thornton, P.E., Running, S.W., and Nemani, R.R. 2000. Parameterization and sensitivity analysis of the BIOME-BGC terrestrial ecosystem model: net primary production controls. *Earth Interactions*, Vol. 4, pp. 1–85.

© 2004 CASI

White, M.A., Nemani, R.R., Thornton, P.E., and Running, S.W. 2002. Satellite evidence of phenological differences between urbanized and rural areas of the eastern United States deciduous broadleaf forest. *Ecosystems*, Vol. 5, pp. 260–273.

Xue, Y., Fennessy, M.J., and Sellers, P.J. 1996. Impact of vegetation properties on U.S. summer weather prediction. *Journal of Geophysical Research, Atmospheres*, Vol. 101, pp. 7419–7430.

Zhou, L., Tucker, C., Kaufmann, R., Slayback, D., Shabanov, N., and Myneni, R. 2001. Variations in northern vegetation activity inferred from satellite data of vegetation index during 1981 to 1999. *Journal of Geophysical Research, Atmospheres*, Vol. 106, pp. 20 069 – 20 083.

Zhou, L., Kaufmann, R.K., Tian, Y., Myneni, R.B., and Tucker, C.J. 2003. Relation between interannual variations in satellite measures of northern forest greenness and climate between 1982 and 1999. *Journal of Geophysical Research, Atmospheres*, Vol. 108, No. 4004.

© 2004 CASI